Eur. Phys. J. D **7**, 487–497 (1999)

THE EUROPEAN PHYSICAL JOURNAL D

EDP Sciences

R-matrix calculation of Raman couplings and dynamical Stark shifts in heavy alkaline-earth atoms

E. Luc-Koenig[1,a], M. Aymar[1], J.-M. Lecomte[1], and A. Lyras[2]

[1] Laboratoire Aimé Cotton, CNRS II, Bâtiment 505, 91405 Orsay Cedex, France
[2] Atomic and Molecular Physics Laboratory, Physics Department, University of Ioannina, 45110 Ioannina, Greece

Received 29 March 1999

Abstract. We report a theoretical approach based on a combination of jj-coupled eigenchannel R-matrix and multichannel quantum-defect (MQDT) methods suitable to determine Raman couplings, dynamical Stark shifts and threshold-resolved ionization rates in heavy alkaline-earth atoms. These atomic parameters are needed to analyze the partial photoelectron spectra and the ionization dynamics of multiphoton processes in a perturbative treatment of the field-atom interaction to the lowest non-vanishing order of perturbation theory. Numerical results are presented in barium, pertaining to the experimental level scheme used by Wang, Chen and Elliott [Phys. Rev. Lett. **77**, 2416 (1996)] to study coherent control through two-color interfering paths. Particular emphasis is given on the comparison of length and velocity formulations for the electric dipole operator.

PACS. 31.15.Ar Ab initio calculations – 32.80.Fb Photoionization of atoms and ions – 32.80.Qk Coherent control of atomic interactions with photons

1 Introduction

Due to the development of intense laser sources, multiphoton ionization (MPI) of multielectron atoms has recently received particular attention from experimentalists and theorists. Multiphoton ionization which occurs *via* closelying near-resonant discrete levels has emphasized the importance of Raman processes and dynamical Stark shifts (also called light shifts), both proportional to the intensity of the laser light [1–6]. Two-photon Raman couplings play also a key role in phenomena such as laser-induced continuum structure (LICS) [7,8] or population transfer through the continuum using processes similar to the stimulated Raman adiabatic passage (STIRAP) [9,10].

The selected theoretical models quoted above concern only alkali atoms. In alkaline-earth atoms, experimental and theoretical studies are scarcer, but the presence of doubly-excited states in the bound or autoionizing energy-range can lead to particularly large Raman couplings. Earlier and recent experiments have demonstrated the importance of Raman couplings in barium using three-photon ionization *via* quasi-degenerate two-photon resonances [11] or using intense picosecond laser pulses [12,13]. The control of photoionization yields into different ionic channels has been investigated in barium by means of two coherent interfering photoionization routes, both being two-photon, two-color pathways resonantly enhanced by an intermediate state [14,15]. In this scheme the two intermediate states are coupled through a Raman process. To interpret the unusual lineshapes observed in that experiment, Nakajima *et al.* [16] have studied the dynamics of a similar system in calcium.

The examples presented above demonstrate the importance of Raman couplings and dynamical Stark shifts and the need for their determination in real atoms. Quantitative studies of MPI processes in multielectron atomic systems are less numerous than in one-active electron systems. Calculations of multiphoton transitions in two-electron atoms have been reviewed recently by Lambropoulos *et al.* [17]. Most of the approaches use L^2-integrable discretized basis sets, such as Slater type orbitals or B-splines, and propose different methods to handle multichannel continuum problems [18–20]. These methods are suitable to study MPI spectra, including energy- or angle-resolved photoelectron spectra, in a perturbative treatment for low or moderate intensity. Some approaches introduce a quantized description of the modes of the electromagnetic field and a formalism based on the resolvent operator. Alternative ones use a classical description of the electromagnetic field coupled to the Bloch equations for the density-matrix or to a perturbative treatment of the time-dependent Schrödinger equation (TDSE). Both approaches can be extended to study near resonant situations by separating in the rotating wave approximation (RWA) [21] the quasi-resonant states from the remaining states of the atom. The latter are eliminated and treated in an effective way through the introduction of atomic

[a] e-mail: koe@sun.lac.u-psud.fr

parameters such as dynamical Stark shifts, ionization widths and Raman-like couplings. Subsequently, these parameters are used to interpret the dynamics of the processes.

For high field strengths, it is no longer possible to separate atomic calculations from the study of the dynamics. Direct non-perturbative solution of the TDSE equation is necessary using either a large atomic basis set or a L^2-discretized basis technique [17]. Another theoretical approach which has been proved to be efficient in the description of MPI processes in multielectron atomic systems is the R-matrix Floquet method introduced by Burke, Francken and Joachain [22]. It expresses the time-dependent wavefunction of the atom as a Fourier series of the harmonics of the frequency of the field, and therefore disregards the pulse shape [22,23].

The applications of both B-spline and R-matrix Floquet methods were restricted to light atomic systems, where the spin-orbit interaction can be disregarded. Theoretical approaches adapted to describe MPI processes in heavy two-electron atom where relativistic effects cannot be neglected are very scarce, even when lowest order perturbation theory is used to account for the field-atom interaction. Several studies have demonstrated that the jj-coupled eigenchannel R-matrix method in combination with the multichannel quantum defect theory (MQDT) [24] can be successfully applied to study single-photon absorption in heavy alkaline-earth atoms. In this approach, electronic correlations as well as spin-orbit interaction are accounted explicitly within the reaction volume. This method has been recently enlarged to the calculation of total and partial two-photon ionization cross-sections [25,26]. The purpose of the present paper is to further extend the eigenchannel jj-coupled R-matrix/MQDT method to the calculation of two-photon atomic parameters, such as Raman couplings and dynamical Stark shifts occurring at the second-order of the perturbation theory in the treatment of the field-atom interaction. Moreover, being coupled to the MQDT method, the eigenchannel R-matrix method is very well-adapted to the determination of threshold-resolved quantities such as the threshold-resolved ionization rates. The numerical results presented in this work, correspond to atomic parameters required in the analysis of coherent control through interfering paths in barium [14,15]. A more complete analysis dealing with the spectroscopic properties involved in this system and the dynamics of this process will be presented in a forthcoming paper [27].

The main points of the method, initially devoted to the interpretation of one-photon photoionization spectra, are recalled in Section 2 and applied to the determination of threshold-resolved atomic quantities. In Section 3, the calculation of Raman couplings and light shifts is presented in detail. Section 4 is focused on a discussion about results obtained using the length or velocity gauge for the electric dipole operator. Indeed, the method based on a frozen-core model excludes completely core-excited intermediate states from the calculation of dynamical Stark shifts and Raman couplings. As a result, the usual equivalence between length and velocity gauges is no longer valid. To our knowledge, comparison of length and velocity formulations in frozen-core models has never been presented. Furthermore, in the so-called Λ or V systems, the discrete states resonantly coupled by the radiation field are explicitly introduced in the Bloch equations governing the time evolution of the system and excluded from the infinite summations involved in atomic parameters introduced at the second-order of atom-field interaction. This complicates and makes more subtle the comparison between length and velocity results.

2 Eigenchannel R-matrix method combined with MQDT: determination of threshold-resolved ionization rates

The present work is devoted to the calculation of the atomic parameters involved in the dynamical analysis [16] of the coherent control of ionization process experimentally studied in barium [14,15]. The $6s^2\ ^1S_0$ ground state and the $6s6p$ and $6s7p\ ^1P_1$ intermediate states, with energies 0, $\hbar\varpi_1$ and $\hbar\varpi_2$ respectively, are denoted in the following as the $|0\rangle$, $|1\rangle$ and $|2\rangle$ states. The state $|1\rangle$ (resp. $|2\rangle$) is near resonantly excited from the $|0\rangle$ state by a laser with angular frequency ω_1, ($\omega_1 \sim \varpi_1$) polarization ϵ_1 and intensity I_1 (resp. ω_2, ϵ_2, I_2 with $\omega_2 \sim \varpi_2$) and then photoionized by a second laser characterized by ω_2, ϵ_2, I_2 (resp. ω_1, ϵ_1, I_1). The two two-photon ionization pathways starting from the state $|0\rangle$ reach the same final continuum states, therefore this ionization process is "coherent" and there is an interference between the two ionization processes *via* $|1\rangle$ or $|2\rangle$. Studying in the RWA approximation the dynamics of this system on the subspace spanned by the three bound states introduces as atomic parameters the one-photon Rabi couplings Ω_i between the ground state and the two intermediate states, the one-photon ionization rates $\gamma_i^{\rm coh}$ from the intermediate states, the dynamical Stark shifts Ω_{ii} of these states and the Raman coupling Ω_{21} between the two intermediate states.

Let us remark, that the method presently developed can also be applied to determine the coherent ionization rates $\gamma_i^{\rm coh}$, the dynamical Stark shifts Ω_{ii} and the Raman coupling Ω_{21} for the $6s6p$ and $6s7p\ ^1P_1$ states of barium, for non-resonant laser lights $\omega_1 \neq \varpi_1$ and $\omega_2 \neq \varpi_2$, but satisfying $\varpi_1 + \omega_2 = \varpi_2 + \omega_1 = E_{\rm f}$. In this later case the $|0\rangle, |1\rangle$ and $|2\rangle$ states are not linked in a so-called V coupling scheme and the corresponding energy-dependence of the atomic parameters can be studied.

2.1 Eigenchannel R-matrix + MQDT method

The calculations performed in barium use a model Hamiltonian to describe the wavefunctions of the two valence electrons outside a frozen Ba^{2+} core. The interaction of each valence electron with the core is described by a ℓ-dependent potential including screening, polarization

and spin-orbit terms [24,28]. Electron correlations are treated within a finite spherical volume V of radius r_o using discrete sets of two-electron basis functions. These functions are antisymmetrized products of one-electron orbitals of definite total angular momentum J and parity π, the core orbitals $1s$ to $5p$ being disregarded. Consequently core excitation effects are not explicitly introduced, although some contributions are implicitly taken into account through the polarization term present in the Hamiltonian. Standard diagonalization of the two-electron Hamiltonian in a finite basis provides the wavefunctions for low-lying levels, while the eigenchannel jj-coupled R-matrix approach is used to study highly excited states.

The $6s^2\ ^1\mathrm{S}_0$ and $6s6p$ and $6s7p\ ^1\mathrm{P}_1$ states are assumed to be confined within the volume V. The size of V should be large enough to include the $6s7p$ state. In the length formulation, convergent computation of the dipole matrix elements for excitation from the $6s7p$ state requires a large reaction volume $r_0 = 50$ a.u., while in the velocity formulation a smaller radius, *i.e.* 40 a.u., is sufficient. In the following we adopt the value $r_0 = 50$ a.u., which allows comparison between calculations using both formulations for the electric dipole operator. The wavefunctions of the bound states are determined as the eigenvectors of the two-electron Hamiltonian matrices $H_{\mathrm{cc}}^{\pi\,J}$ built on large basis sets of functions, denoted as "closed-type" functions, which have vanishing amplitudes on the surface of the finite volume. The maximum ℓ-value for the angular momentum of the monoelectronic wavefunctions used in the basis set is equal to 6, and for a given ℓ-value up to 20 different "closed-type" orbitals are included to ensure convergence. For $J = 0^{\mathrm{e}}$ 1098 functions are used and 2733 for $J = 1^{\mathrm{o}}$. The "closed-type" functions account for various electron correlation, relaxation and polarization effects which take place within the volume V. It must be emphasized that, in the frozen-core approach, these functions do not form a complete set, because they span only the subspace orthogonal to the Ba^{2+} core orbitals.

The final even-parity states reached by absorption of the two photons ω_1 and ω_2 from the ground state lie above the Ba^+ $5d_{5/2}$ threshold in the energy-range close to $\hbar\varpi_1 + \hbar\varpi_2 \approx 50\,607\ \mathrm{cm}^{-1}$. The description of the $J = 0^{\mathrm{e}}, 1^{\mathrm{e}}$ and 2^{e} autoionizing levels is obtained by using the eigenchannel jj-coupled R-matrix approach combined to the MQDT [24,28]. In the eigenchannel R-matrix approach, the wavefunctions of the valence electrons outside the frozen Ba^{2+} core are determined variationally within a finite reaction volume V. The volume of radius $r_0 = 50$ a.u., used to describe the $6s^2\ ^1\mathrm{S}_0$, the $6s6p$ and $6s7p\ ^1\mathrm{P}_1$ bound levels has to be also employed to perform R-matrix calculations of the final autoionizing states. In order to treat the escape of a single electron from the reaction volume into N open or closed MQDT fragmentation channels, the variational basis set includes two-electron "open-type" functions having non-vanishing amplitude on the surface of the reaction volume, in addition to a large set of "closed-type" functions allowing short-range correlation effects to be accounted for. In the present calculation, three "open-type" two-electron basis functions are included to describe ionization in a given channel. Convergence in the description of correlation effects in the final even-parity states is obtained for a relatively small reaction volume $r_0 \sim 25$ to 30 a.u. To ensure convergence of the variational calculations for $r_0 = 50$ a.u. large basis sets are used, with 1107 functions for $J = 0^{\mathrm{e}}$, 2769 for $J = 1^{\mathrm{e}}$ and up to 4150 functions for the $J = 2^{\mathrm{e}}$ symmetries. The parameters finally chosen to generate the two-electron basis set are optimum. Further increase in the reaction volume size, the maximum angular momentum or the number of "closed-type" orbitals would not improve the convergence. The variational calculation gives the logarithmic derivatives at the surface of the reaction volume of N independent solutions of the Schrödinger equation. The eigenchannel MQDT formulation [29,30] is used to extend the wavefunctions obtained in the R-matrix treatment outside the reaction volume, by imposing appropriate boundary conditions at large r.

The even-parity channels converging to the Ba^+ $6s$, $5d_{3/2}$ and $5d_{5/2}$ thresholds are treated as open channels in the MQDT treatment. This treatment involves three even-parity jj-coupled channels for $J = 0^{\mathrm{e}}$, eight for $J = 1^{\mathrm{e}}$ and 11 for $J = 2^{\mathrm{e}}$. Although the $6p7p$ levels [31] lie in the same energy range, no closed channel converging to the $6p$ thresholds was introduced in the MQDT treatment. Indeed, for $r_0 = 50$ a.u., the low-lying $6p7p$ levels fit entirely within the R-matrix box. An efficient way for handling these levels is to use the method developed by Lecomte *et al.* [32], which amounts assuming that the $6p7p$ levels are bound levels included within V and treating directly their interaction with the open continua.

In the autoionizing range, the number of physical solutions is equal to N_0, the number of open channels. In the present study, where no closed channel is introduced, for each final states J^{e}-value one has $N_0 = N$. To calculate the branching ratios corresponding to the photoionization process in each channel $i \equiv \{N_{\mathrm{c}}\ell_{\mathrm{c}}j_{\mathrm{c}},\ \epsilon'\ell'j'\,J\}$, we use the "incoming wave" normalization condition to determine N_0 linearly independent physical solutions denoted $|\psi_i^-(E,J)\rangle = |N_{\mathrm{c}}\ell_{\mathrm{c}}j_{\mathrm{c}},\ \epsilon'\ell'j'J\rangle$ [33].

2.2 Threshold-resolved coherent decay rates and interference terms in the ionization process

This section deals only with the threshold-resolved coherent ionization rates of states $|1\rangle$ and $|2\rangle$ and with the interference terms occurring in the ionization process whose determination requires the calculation of one-photon dipole matrix elements. The calculation of light shifts and two-photon Raman couplings will be addressed in the next section.

The threshold-resolved coherent decay rates of states $|1\rangle$ and $|2\rangle$ associated with $J = 0^{\mathrm{e}}$, 1^{e} or 2^{e} final states are calculated at the resonant energy $E_{\mathrm{r}} = \hbar\varpi_1 + \hbar\varpi_2$. The one-photon dipole reduced matrix element connecting the $6snp\ ^1\mathrm{P}_1$ ($n = 6$ or 7) states to the final channel i with $J = 0^{\mathrm{e}}$, 1^{e} or 2^{e} is defined by:

$$D_i^-(n,E,J) = \langle\psi_i^-(E,J)||\mathbf{D}||\psi(6snp\ ^1\mathrm{P}_1)\rangle, \qquad (1)$$

where the wavefunctions of $6snp\ ^1\mathrm{P}_1$ ($n = 6$ or $n = 7$) states are eigenvectors of $H_{\mathrm{cc}}^{\pi\,J}$ for $J = 1^{\mathrm{o}}$. In equation (1), $\mathbf{D}$ is the electric dipole operator, either in the length $\mathbf{D}^{\mathrm{r}} = \mathbf{r}$ or in the velocity $\mathbf{D}^{\nabla} = \pm\nabla/\hbar\omega$ form, (the upper sign corresponds to an emission process and the lower one to an absorption process) and ω is the frequency of the laser light. From equation (1) the following threshold-resolved resonant quantities at energy E_{r} are calculated:

$$\mathcal{D}(N_{\mathrm{c}}\ell_{\mathrm{c}}j_{\mathrm{c}}, n, n', J) = \sum_{i'} \pi\, D^{-}_{i'}(n, E_{\mathrm{r}}, J) D^{-*}_{i'}(n', E_{\mathrm{r}}, J), \tag{2}$$

where * denotes the complex conjugate and the sum runs over all channels $i' \equiv \{N_{\mathrm{c}}\ell_{\mathrm{c}}j_{\mathrm{c}},\ \epsilon'\ell'j'\}$ associated with the $\mathrm{Ba}^+\,(N_{\mathrm{c}}\ell_{\mathrm{c}}j_{\mathrm{c}})$ ionization threshold. By introducing the polarizations of the laser lights and by summing over the J values of the final states, ($J = 0^{\mathrm{e}}, 2^{\mathrm{e}}$ for linear parallel polarizations and $J = 1^{\mathrm{e}}, 2^{\mathrm{e}}$ for perpendicular linear polarizations), we determine the threshold-resolved coherent ionization rates and the threshold-resolved interference terms between the two ionization paths *via* states $|1\rangle$ or $|2\rangle$. These quantities are linear combinations of $\mathcal{D}$ with coefficients $a_J\, I_k$ and $b_J\sqrt{I_1\, I_2}$, where a_J and b_J are angular coefficients depending on the polarizations of the lasers.

The coherent threshold-resolved ionization rate for the state j ionized by the laser light k is:

$$\begin{aligned}\frac{1}{2}\gamma_j^{\mathrm{coh}}(N_{\mathrm{c}}\ell_{\mathrm{c}}j_{\mathrm{c}}) &= \sum_J \frac{1}{2}\gamma_j^{\mathrm{coh}}(N_{\mathrm{c}}\ell_{\mathrm{c}}j_{\mathrm{c}}; J)\\ &= \sum_J a_J I_k \mathcal{D}(N_{\mathrm{c}}\ell_{\mathrm{c}}j_{\mathrm{c}}, n, n, J),\end{aligned} \tag{3}$$

with $n = n' = 6$ or 7 ($j = 1$ or 2) and $k \neq j$. Note that the summation of $\gamma_j^{\mathrm{coh}}(N_{\mathrm{c}}\ell_{\mathrm{c}}j_{\mathrm{c}})$ over the $N_{\mathrm{c}}\ell_{\mathrm{c}}j_{\mathrm{c}}$ thresholds gives the total coherent rate γ_j^{coh}.

The threshold-resolved interference term between ionization paths *via* intermediate states $|1\rangle$ and $|2\rangle$ is:

$$\begin{aligned}\gamma_{21}^{\mathrm{coh}}(N_{\mathrm{c}}\ell_{\mathrm{c}}j_{\mathrm{c}}) &= \sum_J \gamma_{21}^{\mathrm{coh}}(N_{\mathrm{c}}\ell_{\mathrm{c}}j_{\mathrm{c}}; J)\\ &= \sum_J b_J\sqrt{I_1 I_2}\mathcal{D}(N_{\mathrm{c}}\ell_{\mathrm{c}}j_{\mathrm{c}}, n, n', J),\end{aligned} \tag{4}$$

with $n = 6$ and $n' = 7$. The $\gamma_{21}^{\mathrm{coh}}(N_{\mathrm{c}}\ell_{\mathrm{c}}j_{\mathrm{c}})$ coefficients are complex numbers satisfying $\gamma_{21}^{\mathrm{coh}}(N_{\mathrm{c}}\ell_{\mathrm{c}}j_{\mathrm{c}}) = \gamma_{12}^{\mathrm{coh}\,*}(N_{\mathrm{c}}\ell_{\mathrm{c}}j_{\mathrm{c}})$. As a result to the normalization condition, summation of their imaginary parts over the $N_{\mathrm{c}}\ell_{\mathrm{c}}j_{\mathrm{c}}$ thresholds is equal to zero.

Let us remark that the threshold-resolved interference terms have been called "two-photon Rabi frequencies from $|1\rangle$ and $|2\rangle$ through the continuum associated with the ionization threshold $N_{\mathrm{c}}\ell_{\mathrm{c}}j_{\mathrm{c}}$" in an earlier work [16].

The values obtained for the coherent threshold-resolved ionization rates for the $6s6p$ and $6s7p$ states of barium and the threshold-resolved interference terms are given in Table 1. Length and velocity results are presented and the linear polarizations of the lasers are either parallel or perpendicular as in the experiment [14,15]. The values for the Rabi frequencies, Ω_i ($i = 1$ or 2), for the resonant transitions coupling the state $|0\rangle$ to the intermediate states $|1\rangle$ and $|2\rangle$ are also given. These one-photon parameters are proportional to $\sqrt{I_i}$. This table contains also two-photon atomic parameters, which will be discussed below.

For all the resonant one-photon atomic parameters, the values calculated using either the length or the velocity formulation of the dipole transition operator agree to within less than 10%. It can be verified from Table 1 that the sum over the three ionization thresholds of the imaginary parts of the threshold-resolved interference terms strictly vanishes.

3 Two-photon Raman couplings and light shifts

Light shifts and two-photon Raman couplings appear to the second order of perturbation theory. They correspond to scattering-like processes, during which one photon is emitted and another one is absorbed. The process where absorption occurs before emission is called in the present paper the "rotating" one, as in [5], the "counter-rotating" process corresponding to stimulated emission followed by absorption. Both processes could be significant [8] and involve summations over bound and continuum states. When the energy reached after absorption of the photon is greater than the first ionization limit, the denominator y involved in the summation vanishes in the integration range. Thus, the "rotating" contribution separates into an imaginary part corresponding to the "resonant" continuum intermediate states with energy $E_{\mathrm{r}} = \hbar\varpi_1 + \hbar\varpi_2$ and a real part associated with the contribution of "non-resonant" intermediate states with energy $E \neq E_{\mathrm{r}}$. These terms result from the well-known formula:

$$\lim_{\eta\to 0_+} \frac{1}{y + \mathrm{i}\eta} = \mathcal{P}\frac{1}{y} - \mathrm{i}\pi\delta(y), \tag{5}$$

where $\mathcal{P}$ denotes the Cauchy principal part and where the contributions of the imaginary term are expressed in terms of one-photon dipole matrix elements calculated at the resonant energy where y vanishes.

3.1 Two-photon Raman couplings

The two-photon Raman coupling Ω_{21} between the $6s6p\ ^1\mathrm{P}_1$ and $6s7p\ ^1\mathrm{P}_1$ states, results from two processes:

(i) absorption by the state $|1\rangle$ of the photon ω_2 with polarization ϵ_2 leading to the virtual states $|E_X\, J\rangle$, followed by stimulated emission of the photon ω_1 with polarization ϵ_1, towards state $|2\rangle$. The contribution

Table 1. Atomic parameters for the three-state model pertaining to the experimental scheme used to study coherent control of the photoionization products in barium [14,15]. The Rabi couplings, Raman coupling and the dynamical Stark shifts are expressed in rad s^{-1}, and the ionization rates and the interference terms in s^{-1}. The two lasers have parallel or perpendicular linear polarizations and the intensities I_i are expressed in W cm^{-2}. These parameters are calculated using the length r or the velocity ∇ formulation for the electric dipole operator. Ω_i: one-photon Rabi frequency between the ground state and the two excited states $|i\rangle$ $i = 1, 2$; Ω_{21}: two-photon Raman coupling between states $|1\rangle$ and $|2\rangle$; $\gamma_{21}^{\rm coh}(N_{\rm c}\ell_{\rm c}j_{\rm c})$: threshold-resolved interference term in the ionization from the ground state *via* the excited state $|1\rangle$ and $|2\rangle$; Ω_{ii}: dynamical Stark shift and ionization width for the state $|i\rangle$ in the presence of the laser light k; $\gamma_i^{\rm coh}(N_{\rm c}\ell_{\rm c}j_{\rm c})$: threshold-resolved coherent ionization rate for the state $|i\rangle$ in the presence of the laser light k.

polarization	$\parallel$	$\parallel$	$\perp$	$\perp$
formulation	r	∇	r	∇
$\Omega_1/\sqrt{I_1}$	3.627×10^8	3.716×10^8	3.627×10^8	3.716×10^8
$\Omega_2/\sqrt{I_2}$	-9.490×10^7	-9.868×10^7	9.490×10^7	9.868×10^7
$\Omega_{21}/\sqrt{I_1 I_2}$	$-31.52 - \mathrm{i}\,1.13$	$-16.95 - \mathrm{i}\,1.32$	$86.43 - \mathrm{i}\,11.68$	$77.22 - \mathrm{i}\,13.04$
$\gamma_{21}^{\rm coh}(6s_{1/2})/\sqrt{I_1 I_2}$	$-0.07 - \mathrm{i}\,2.72$	$0.16 - \mathrm{i}\,2.52$	$6.99 + \mathrm{i}\,1.29$	$7.74 + \mathrm{i}\,1.18$
$\gamma_{21}^{\rm coh}(5d_{3/2})/\sqrt{I_1 I_2}$	$0.50 + \mathrm{i}\,1.10$	$0.52 + \mathrm{i}\,1.03$	$5.25 - \mathrm{i}\,0.71$	$5.83 - \mathrm{i}\,0.70$
$\gamma_{21}^{\rm coh}(5d_{5/2})/\sqrt{I_1 I_2}$	$0.70 + \mathrm{i}\,1.62$	$0.64 + \mathrm{i}\,1.49$	$-0.56 - \mathrm{i}\,0.58$	$-0.53 - \mathrm{i}\,0.48$
Ω_{11}/I_2	$34.73 - \mathrm{i}\,19.16$	$34.31 - \mathrm{i}\,17.62$	$56.79 - \mathrm{i}\,16.85$	$53.08 - \mathrm{i}\,16.73$
$(1/2)\gamma_1^{\rm coh}(6s_{1/2})/I_2$	16.92	15.54	11.85	11.38
$(1/2)\gamma_1^{\rm coh}(5d_{3/2})/I_2$	1.05	0.92	3.23	3.54
$(1/2)\gamma_1^{\rm coh}(5d_{5/2})/I_2$	1.19	1.16	1.72	1.81
Ω_{11}/I_1	-128.45	-209.46	-128.45	-209.46
Ω_{22}/I_1	$-37.76 - \mathrm{i}\,10.13$	$-56.73 - \mathrm{i}\,10.43$	$277.69 - \mathrm{i}\,58.09$	$277.55 - \mathrm{i}\,61.55$
$(1/2)\gamma_2^{\rm coh}(6s_{1/2})/I_1$	3.62	3.71	39.53	41.85
$(1/2)\gamma_2^{\rm coh}(5d_{3/2})/I_1$	1.86	1.93	15.99	17.19
$(1/2)\gamma_2^{\rm coh}(5d_{5/2})/I_1$	4.65	4.79	2.57	2.51
Ω_{22}/I_2	$31.29 - \mathrm{i}\,8.37$	$23.17 - \mathrm{i}\,9.00$	$31.29 - \mathrm{i}\,8.37$	$23.17 - \mathrm{i}\,9.00$

of this "rotating" process is given by:

$$\frac{\overline{\Omega}_{21}}{\sqrt{I_1 I_2}} = \sum_J \frac{\overline{\Omega}_{21}(J)}{\sqrt{I_1 I_2}} = \sum_J \left[\lim_{\eta \to 0_+} \int \mathrm{d}E_X \frac{\langle 2|\mathbf{D}_1 \cdot \boldsymbol{\epsilon}_1|E_X J\rangle \langle E_X J|\mathbf{D}_2 \cdot \boldsymbol{\epsilon}_2|1\rangle}{\hbar\varpi_1 + \hbar\omega_2 - E_X + \mathrm{i}\eta} \right]. \quad (6)$$

The summation over J in equation (6) includes $J = 0^{\rm e}$, $2^{\rm e}$ states for parallel linear polarizations and $J = 1^{\rm e}$, $2^{\rm e}$ for perpendicular linear polarizations. In equation (6), the integration is meant to include a discrete summation over bound states plus an integration over continuum states. Since the energy $\hbar\varpi_1 + \hbar\omega_2$ is above the first ionization threshold, $\overline{\Omega}_{21}(J)$ is a complex number. The real part corresponds to the Cauchy principal part integral obtained for $\eta = 0$, which accounts for the contribution of nonresonant states $E_X \neq E_{\rm r}$. The imaginary part, due to the resonant continuum states, is $-\pi\langle 2|\mathbf{D}_1 \cdot \boldsymbol{\epsilon}_1|E_{\rm r} J\rangle\langle E_{\rm r} J|\mathbf{D}_2 \cdot \boldsymbol{\epsilon}_2|1\rangle$, where $E_{\rm r} = \hbar\omega_1 + \hbar\varpi_2 \sim \hbar\varpi_1 + \hbar\omega_2$;

(ii) stimulated emission by the state $|1\rangle$ of the photon ω_1 with polarization ϵ_1 leading to the virtual states $|E_{X'} J'\rangle$, followed by absorption towards state $|2\rangle$ of the photon ω_2 with polarization ϵ_2. The two-photon amplitude of this "counter-rotating" process, is given by:

$$\frac{om_{21}}{\sqrt{I_1 I_2}} = \sum_{J'} \int \mathrm{d}E_{X'} \frac{\langle 2|\mathbf{D}_2 \cdot \boldsymbol{\epsilon}_2|E_{X'} J'\rangle \langle E_{X'} J'|\mathbf{D}_1 \cdot \boldsymbol{\epsilon}_1|1\rangle}{\hbar\varpi_1 - \hbar\omega_1 - E_{X'}}. \quad (7)$$

Because the energy $\hbar\varpi_1 - \hbar\omega_1$ involved in equation (7) is close to the ground state energy, om_{21} is a real quantity.

The total two-photon Raman coupling, proportional to $\sqrt{I_1 I_2}$, is equal to:

$$\Omega_{21} = \overline{\Omega}_{21} + om_{21}. \quad (8)$$

3.1.1 Calculation of "rotating" contribution

The "rotating" contribution is proportional to the matrix element: $\langle 2|\mathbf{D}_1 \cdot \boldsymbol{\epsilon}_1\, G(\hbar\varpi_1 + \hbar\omega_2)\, \mathbf{D}_2 \cdot \boldsymbol{\epsilon}_2|1\rangle$, where $G(E) = \lim_{\eta \to 0_+}(E - H + \mathrm{i}\eta)^{-1}$ is the Green operator. As in the R-matrix/MQDT calculation of two-photon transition amplitudes [25,26], explicit summation is avoided by using the approach of Dalgarno and Lewis [34].

For each J-value one determines a wavefunction $\Lambda_{p_1}(J)$, describing the perturbation of state $|1\rangle$ by the laser light ω_2, as the physical solution of the inhomogeneous equation:

$$(\hbar\varpi_1 + \hbar\omega_2 - H)|\Lambda_{p_1}(J)\rangle = (\mathbf{D}_2 \cdot \boldsymbol{\epsilon}_2)|1\rangle, \qquad (9)$$

satisfying outgoing-wave boundary conditions in the open channels and decreasing exponentially in the closed channels. Then:

$$\overline{\Omega}_{21}(J) = \langle 2|\mathbf{D}_1 \cdot \boldsymbol{\epsilon}_1|\Lambda_{p_1}(J)\rangle\sqrt{I_1 I_2}. \qquad (10)$$

In both equations (9, 10) we use the same gauge corresponding either to the length or to the velocity form, which defines two perturbed wavefunctions $\Lambda^{r}_{p_1}(J)$ and $\Lambda^{\nabla}_{p_1}(J)$, solutions of a different second-order differential equation, and two "rotating" contributions $\overline{\Omega}^{r}_{21}(J)$ and $\overline{\Omega}^{\nabla}_{21}(J)$. The gauge-dependence of these functions and of the Raman-coupling coefficients will be discussed in Section 4.

Using the R-matrix/MQDT approach, $\Lambda(J)$ is expanded within the reaction volume on the two-electron basis set from which the core orbitals $1s$ to $5p$ are excluded. Outside V, $\Lambda(J)$ is matched to an analytic expansion in terms of channels functions, used to impose the correct boundary conditions for large r [25].

It is also possible to determine the wavefunction $\Lambda_{p_2}(J)$ describing the state $|2\rangle$ perturbed by the ω_1 laser light and the transition amplitude $\overline{\Omega}_{12}(J)$ towards state $|1\rangle$ under the ω_2 laser light. From equation (6) it is obvious that, when the same formulation for the dipole operator is used, one has $\overline{\Omega}_{12}(J) = \overline{\Omega}_{21}(J)$. In the present work, this equality is numerically satisfied with at least 8 significant digits.

For a given J-value, the imaginary part is related to the contribution of resonant continuum states with the considered J and it can be expressed in terms of one-photon matrix elements. Therefore, it does not depend on the gauge and is numerically equal to within 1%, to the sum over all threshold-resolved interference terms (Eq. (4)). One has:

$$\Im[\overline{\Omega}_{21}(J)] = -\sum_{N_c\ell_c j_c} \gamma^{coh}_{21}(N_c\ell_c j_c; J), \qquad (11)$$

where both quantities are calculated with the same gauge and where the summation in the right hand side gives a real number.

A similar relation remains valid for the imaginary part of the Raman coupling, after summation over J and after adding the "counter-rotating" term, which is real. This property can be verified in Table 1, by comparing $\Im[\Omega_{21}]$ to the sum over the ionization thresholds of the real parts $\Re[\gamma^{coh}_{21}(N_c\ell_c j_c)]$, and by calculating the sum of the imaginary parts $\Im[\gamma^{coh}_{21}(N_c\ell_c j_c)]$. However neither these relations nor the equality $\Omega_{12} = \Omega_{21}$ were satisfied in the atomic parameters obtained for calcium [16].

3.1.2 Calculation of "counter-rotating" contribution

The om_{21} term, introduced in equation (7), would be obtained from perturbed functions similar to the $\Lambda_{p_1}(J)$ ones (Eq. (9)), but calculated at the energy $\hbar\varpi_1 - \hbar\omega_1 \sim 0$. At this energy, all channels are closed. Using a large reaction volume with radius $r_0 = 50$ a.u. would introduce numerical difficulties related to the exponential growth of the Coulomb wavefunctions f and g [29,30] in the closed channels. An alternative to the Dalgarno and Lewis method is to obtain directly the expansion of the Green operator $G(\hbar\varpi_1 - \hbar\omega_1)$. Thus om_{21} is calculated by performing an explicit summation over all the eigenstates of the Hamiltonian matrix $H^{\pi\, J'}_{cc}$ for $J' = 0^e$ and $J' = 2^e$ built on basis states contained within V and representing bound states as well as discretized continuum states with a given J' value, the latter being located below as well above the double ionization limit Ba^{2+}.

3.2 Calculation of light shifts

The light shifts, or dynamical Stark shifts, $\Omega_{ii}(\omega_k)$ of the bound states $|i\rangle$ due to the laser light ω_k ($k = 1$ or $k = 2$), proportional to I_k are calculated in the same way as Ω_{12} using the relation $\Omega_{ii} = \overline{\Omega}_{ii} + om_{ii}$, but with $\mathbf{D}_1 \cdot \boldsymbol{\epsilon}^*_1 = \mathbf{D}_2 \cdot \boldsymbol{\epsilon}_2$. However, now in the velocity formulation, the contribution of the $\mathbf{A}^2_k$ term proportional to the square of the vector potential associated with laser k is to be added to the "rotating" and "counter-rotating" terms. Indeed, the $\mathbf{A}^2_k$ term which appears to the first order of perturbation theory is also proportional to the laser intensity I_k. One has:

$$\tilde{\Omega}^{\nabla}_{ii}(\omega_k) = \Omega^{\nabla}_{ii}(\omega_k) + \frac{\mathbf{A}^2_k}{2\omega^2_k}2\mathcal{N}, \qquad (12)$$

where $\mathcal{N} = 2$ is the number of valence electrons treated in the frozen-core model. For $\hbar\varpi_i + \hbar\omega_k$ greater than the first ionization limit $\Omega_{ii}(\omega_k)$ is a complex number whose real part is equal to the light shift and the imaginary part to the opposite of the total ionization rate. The imaginary parts of $\Omega_{ii}(\omega_k)$ satisfies, for $i \neq k$, the following relation which is numerically verified within a few %, as it can be seen in Table 1

$$\Im[\Omega_{ii}(\omega_k)] = -\frac{1}{2}\sum_{N_c\ell_c j_c} \gamma^{coh}_{i}(N_c\ell_c j_c). \qquad (13)$$

3.3 Energy dependence of the Raman coupling

Raman coupling can be defined in the presence of two lasers with angular frequencies $\omega_1 \neq \varpi_1$ and $\omega_2 \neq \varpi_2$ but satisfying $E_f = \varpi_1 + \omega_2 = \varpi_2 + \omega_1$. This scattering process corresponds to resonant continuum states with energy E_f. The energy variations of the real and imaginary parts of the Raman coupling $\Omega_{21}(E_f)$ calculated using the length form for the electric dipole operator, are presented in Figure 1, for laser lights with parallel (Fig. 1a) or perpendicular (Fig. 1b) linear polarizations. Since state $|0\rangle$ is introduced in the calculation of the "counter-rotating" term for this non-resonant Raman coupling, there is a divergence at the resonant energy E_r. The studied energy-range

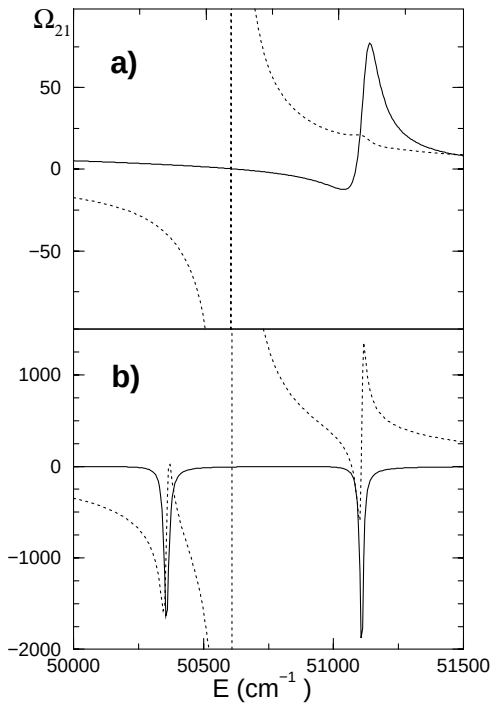

Fig. 1. Energy variation for the Raman coupling $\Omega_{21}(E_\mathrm{f})$ with $E_\mathrm{f} = \hbar(\varpi_1+\omega_2) = \hbar(\varpi_2+\omega_1)$ between the $6s6p\ ^1\mathrm{P}_1$ state, with energy $\hbar\varpi_1$, and the $6s7p\ ^1\mathrm{P}_1$ state, with energy $\hbar\varpi_2$, of barium in presence of laser lights with linear parallel polarizations (Fig. 1a) or linear perpendicular polarizations (Fig. 1b) and angular frequencies ω_1 and ω_2. Dashed line: $\Re[\Omega_{21}]$ (divided by a factor 20 in (a)), which diverges at $E_\mathrm{r} = \hbar(\varpi_1 + \varpi_2)$, due to the contribution from the $6s^2$ state to the "counter-rotating" interaction. Full line: $\Im[\Omega_{21}]$. The resonances correspond to the $6p7p$ autoionizing states with $J = 2$ (a) and $J = 1$ (b) [31].

includes the lower lying $6p7p$ autoionized resonances [31]. A detailed analysis of these resonances will be presented in a forthcoming paper [27]. For perpendicular polarizations (Fig. 1b) the energy dependence is dominated by the $6p7p\ ^1\mathrm{P}_1$ and $^3\mathrm{D}_1$ narrow resonances at respectively 50 383 cm^{-1} and 51 113 cm^{-1}, which appear as Lorentzian-like (resp. dispersion-like) profiles in the imaginary (resp. real) part of the Raman coupling coefficient. With parallel polarizations (Fig. 1a) the broad $6p7p\ ^3\mathrm{D}_2$ resonance, excited near 51 200 cm^{-1}, gives rise to Fano-like profiles in the real and in the imaginary part of Ω_{21}. Larger values for the Raman coupling are observed near the resonances. To study the dynamics of the system in this energy range, the three state model is no longer valid. To extend this model, it is necessary to explicitly introduce the autoionizing states in the effective Hamiltonian.

In Figure 1, where the states are non-resonantly coupled by the laser lights, the Raman couplings and light shifts obtained by introducing all intermediate states in the summations do not depend significantly on the gauge used.

4 Raman coupling and dynamical Stark shifts in a V system

In the particular case where the $|1\rangle$ and $|2\rangle$ states are resonantly coupled through a state $|0\rangle$ in a V (resp. Λ) scheme, the resonant state $|0\rangle$ is to be excluded from the "counter-rotating" (resp. "rotating") term in the calculation of Raman couplings and dynamical Stark shifts. The atomic parameters obtained in this way have by themselves no physical meaning. Introduced in a dynamical study, they represent the coupling between states $|1\rangle$ and $|2\rangle$ and the shifts of these states due to all non-resonant states. Therefore the $|0\rangle$ state is excluded from the summations in the calculation of atomic parameters involved in the interpretation of the coherent control experiment [14,15], and given in Tables 1, 2 and 3. In this section we discuss Raman couplings and light shifts for states $|1\rangle$ and $|2\rangle$ resonantly coupled through a state $|0\rangle$ in a V scheme, as in the coherent control experiment [14,15]. In this case the $|0\rangle$ state is excluded from the "counter-rotating" contribution. A special emphasis is given to the comparison of length and velocity formulations.

4.1 Relative contributions of "rotating" and "counter-rotating" interactions

Table 2 presents the contributions of the "rotating" (a) and "counter-rotating" (b) terms to the two-photon Raman coupling and to the dynamical Stark shifts in the length $\Omega^\mathrm{r}_{ij}/\sqrt{I_iI_j}$ and velocity forms $\Omega^\nabla_{ij}/\sqrt{I_iI_j}$. Comparing ($a$) and S = (a) + (b) demonstrates that the "counter-rotating" interaction cannot be disregarded. The importance of this term in LICS has been emphasized by Dai and Lambropoulos [8] who called it "stimulated Raman coupling". Furthermore, comparing the length and velocity values for the "rotating" or "counter-rotating" term proves that it is meaningless to analyze separately each process, both contributing simultaneously to the same scattering-like interaction. The comparison between length and velocity values for the sum S will be discussed below.

4.2 Raman couplings and dynamical Stark shifts

Table 1 reports the values of the Raman couplings and light shifts pertaining to the interpretation of Wang *et al.* experiment [14,15]. The values obtained with length and velocity formulations are presented for parallel and perpendicular polarizations.

For the laser intensities used in the experiment [15], $I_1 \sim 8\times10^6$ W cm^{-2} and $I_2 \sim 1\times10^6$ W cm^{-2}, the one-photon Rabi frequencies $\Omega_1 \sim 5$ cm^{-1} and $\Omega_2 \sim 0.5$ cm^{-1} are about 10^4 to 10^5 times larger than the ionization widths, which are of the order of 1×10^{-4} cm^{-1}. The Raman couplings and the ionization rates are of the same order of magnitude but these two atomic parameters are smaller than the Rabi frequencies, which appear to first order in the atom-field interaction.

Table 2. Contributions of the "rotating" (a) and "counter-rotating" (b) terms and of their sum $S = (a) + (b)$ to the real parts of the two-photon Raman couplings ($i \neq j$) and to the dynamical Stark shifts ($i = j$) in the length $\Omega^{\rm r}_{ij}$ and velocity Ω^{∇}_{ij} formulations, for parallel or perpendicular linear polarizations.

pol.	$i\,j$	$\Re(\Omega^{\rm r}_{ij})/\sqrt{I_iI_j}$			$\Re(\Omega^{\nabla}_{ij})/\sqrt{I_iI_j}$		
		(a)	(b)	S	(a)	(b)	S
$\parallel$	2 1	−3.1	−28.4	−31.5	−23.8	6.9	−16.9
$\parallel$	1 1	119.4	−84.7	34.7	34.1	−26.9	7.2
$\parallel$	2 2	467.4	− 505.2	−37.8	− 130.2	−14.8	− 145.0
$\perp$	2 1	76.2	10.2	86.4	79.2	−2.0	77.2
$\perp$	1 1	74.3	−17.4	56.9	32.9	−6.9	26.0
$\perp$	2 2	461.3	−183.6	277.5	203.1	−13.9	189.2

Table 3. Real parts of the two-photon Raman couplings ($i \neq j$) and dynamical Stark shifts ($i = j$) due to photon ω_k ($k \neq i$) in the velocity form $\widetilde{\Omega}^{\nabla}_{ij}$ or in the length form $\Omega^{\rm r}_{ij}$ for parallel or perpendicular linear polarizations. Ω^{∇}_{ij} and $\Omega^{\rm r}_{ij}$: sums of the "rotating" and "counter-rotating" contributions; $\mathcal{N}/\omega_k^2$: in the velocity form, contribution to first order of perturbation theory of the interaction quadratic in the potential vector $\mathbf{A}$; total $= \Re(\Omega^{\rm r}_{ij})/\sqrt{I_iI_j} + (a) + (b) + (c)$: total value of the second member of equation (18) which is to be compared with the first member $\Re(\Omega^{\nabla}_{ij})/\sqrt{I_iI_j}$; (a) and (b): contributions to the differences between velocity and length values due to the incompleteness of the basis set used in the R-matrix treatment; (c): contribution to the difference between velocity and length values due to the exclusion of the ground state from the "counter-rotating" contribution.

pol.	$i\,j$	$\frac{\Re(\Omega^{\nabla}_{ij})}{\sqrt{I_iI_j}}$	$\frac{\mathcal{N}}{\omega_k^2}$	$\frac{\Re(\widetilde{\Omega}^{\nabla}_{ij})}{\sqrt{I_iI_j}}$	$\frac{\Re(\Omega^{\rm r}_{ij})}{\sqrt{I_iI_j}}$	(a)	(b)	(c)	total
$\parallel$	2 1	−16.9		−16.9	−31.5	0.0	−0.3	+16.0	−15.7
$\parallel$	1 1	+7.2	+27.1	+34.3	+34.7	0.0	−28.5	0.0	+6.3
$\parallel$	2 2	−145.0	+88.3	−56.7	−37.8	0.0	−104.0	0.0	−141.8
$\perp$	2 1	+77.3		+77.3	+86.4	+ 0.77	−0.41	− 16.0	+70.8
$\perp$	1 1	+26.0	+27.1	+53.1	56.9	0.0	−33.0	0.0	+23.9
$\perp$	2 2	+ 189.2	+ 88.3	+ 277.5	277.7	0.0	− 104.2	0.0	173.5

4.3 Comparison between length and velocity formulations

In this section we compare length and velocity formulations for calculation of Raman couplings and light shifts for the states $|1\rangle$ and $|2\rangle$ resonantly coupled through the state $|0\rangle$ in a V scheme, as in the coherent control experiment [14,15]. In this case the $|0\rangle$ state is excluded from the "counter-rotating" contribution.

Equivalence of the two forms, length and velocity, for the calculation of a non-resonant two-photon scattering process is presented by Cohen-Tannoudji *et al.* [35] (Sect. $\mathrm{E}_{IV.7}$). The energies of the initial $\hbar\varpi_1$ and final $\hbar\varpi_2$ states are related to the angular frequencies of the absorbed ω_2 and emitted ω_1 photons by $\varpi_1 + \omega_2 = \varpi_2 + \omega_1$. This process is non-resonant inasmuch as there is no discrete state in the system reached during the scattering process. Equivalence is obtained when "rotating" and "counter-rotating" contributions are added, and when summation over all J-values for the intermediate states is included.

The demonstration is based on the equality between the matrix elements of the one-photon dipole transition operator either in the length or in the velocity form, evaluated between exact eigenstates of a non-relativistic Hamiltonian:

$$\langle a|\boldsymbol{\nabla}\cdot\boldsymbol{\epsilon}|b\rangle = (E_b - E_a)\langle a|\mathbf{r}\cdot\boldsymbol{\epsilon}|b\rangle, \qquad (14)$$

where E_a and E_b are the eigenvalues associated with the eigenstates $|a\rangle$ and $|b\rangle$.

In the present approach where a model Hamiltonian including the spin-orbit interaction is introduced, the equivalence between the two gauges is only approximate. However comparison of the values for the one-photon dipole matrix elements in the length or velocity forms (Sect. 2.2) demonstrates that the spin-orbit term has only a weak influence, generally less than 5%.

Furthermore to suppress summations over intermediate states, Cohen-Tannoudji *et al.* [35] utilize the closure

$$\frac{\Omega_{21}^{\nabla}}{\sqrt{I_1 I_2}} = \frac{\Omega_{21}^{\rm r}}{\sqrt{I_1 I_2}} - \frac{1}{\omega_1}\sum_{E_X\,J}[\langle 2|\mathbf{D}^{\rm r}\cdot\boldsymbol{\epsilon}_2|E_X J\rangle\langle E_X J|\mathbf{D}^{\rm r}\cdot\boldsymbol{\epsilon}_1|1\rangle - \langle 2|\mathbf{D}^{\rm r}\cdot\boldsymbol{\epsilon}_1|E_X J\rangle\langle E_X J|\mathbf{D}^{\rm r}\cdot\boldsymbol{\epsilon}_2|1\rangle]$$
$$- \frac{1}{\omega_1\omega_2}\sum_{E_X\,J}[\langle 2|\mathbf{D}^{\nabla}\cdot\boldsymbol{\epsilon}_2|E_X J\rangle\langle E_X J|\mathbf{D}^{\rm r}\cdot\boldsymbol{\epsilon}_1|1\rangle - \langle 2|\mathbf{D}^{\rm r}\cdot\boldsymbol{\epsilon}_1|E_X J\rangle\langle E_X J|\mathbf{D}^{\nabla}\cdot\boldsymbol{\epsilon}_2|1\rangle]$$
$$- \frac{\omega_1+\omega_2}{\omega_1\omega_2}\langle 2|\mathbf{D}^{\rm r}\cdot\boldsymbol{\epsilon}_2|0\rangle\langle 0|\mathbf{D}^{\rm r}\cdot\boldsymbol{\epsilon}_1|1\rangle \qquad (18)$$

relation $\sum_{E_X\,J}|E_X J\rangle\langle E_X J| = 1$ which is not valid for the calculations presented in the present work. Indeed, the basis set introduced in the R-matrix calculation spans a non-complete space, the subspace orthogonal to the Ba^+ core orbitals, and the ground state $6s^2$ is excluded from the "counter-rotating" contributions to the Raman coupling and dynamical Stark shifts.

The non-applicability of the closure relation for the basis set used in the R-matrix calculation can be shown by studying the following identity:

$$\langle i|z^2|j\rangle = \sum_{E_X\,J}\langle i|z|E_X\,J\rangle\langle E_X\,J|z|j\rangle, \qquad (15)$$

where the second member is evaluated by a summation over all eigenstates of $H_{\rm cc}^{\pi\,J}$. In this example, the $6s^2$ state is introduced in the summation. For diagonal quantities $|i\rangle = |j\rangle$ all terms in the summation have positive values and this relation is satisfied to within 15% for $|i\rangle = |1\rangle$ and 2% for $|i\rangle = |2\rangle$. For $|i\rangle = |1\rangle$ and $|j\rangle = |2\rangle$ the terms have different signs, which explains why the corresponding non-diagonal quantity is more sensitive to the incompleteness of the basis; indeed one obtains: $10.6 \neq 7.2$. This comparison points out the incompleteness of the subspace spanned in the summation which is restricted to the subspace orthogonal to the Ba^+ core, but does not give information on the contribution of the $6s^2$ state.

For a given J-value, the perturbed wavefunctions Λ in the length and velocity forms are both calculated in the subspace orthogonal to the core orbitals. They are solutions of the same second order differential equations with different right-hand side (Eq. (9)) and are related by:

$$\Lambda_{\rm p_1}^{\nabla}(J) = - \Lambda_{\rm p_1}^{\rm r}(J) + \frac{1}{\omega_2}\sum_{E_X}|E_X J\rangle\langle E_X\,J\,|\mathbf{D}_2^{\rm r}\cdot\boldsymbol{\epsilon}_2|1\rangle. \qquad (16)$$

From this relation, the following "mixed-gauge" two-photon matrix element can be calculated:

$$\overline{\Omega}_{i1}^{{\rm r}-\nabla}(J) = \langle i|\mathbf{D}_i^{\rm r}\cdot\boldsymbol{\epsilon}_i|\Lambda_{\rm p_1}^{\boldsymbol{\nabla}}(J)\rangle = -\overline{\Omega}_{i1}^{\rm r}(J) + \frac{1}{\omega_2}\sum_{E_X}\langle i|\mathbf{D}_i^{\rm r}\cdot\boldsymbol{\epsilon}_i|E_X\,J\,\rangle \times \langle E_X\,J|\mathbf{D}_2^{\rm r}\cdot\boldsymbol{\epsilon}_2|1\rangle. \qquad (17)$$

In (17), all functions $|\Lambda_{\rm p_1}^{\nabla}(J)\rangle$ and $|E_X J\rangle$, which are eigenstates of $H_{\rm cc}^{\pi\,J}$, are calculated in the subspace orthogonal to the core orbitals. Therefore this equation provides a test of the convergence of the R-matrix calculations for a given J-value but cannot be used to assess the effect of the exclusion of the core orbitals from the basis set. This relation is numerically satisfied with an error smaller than 5% for each J-value separately, which proves that our basis set is sufficiently large to correctly describe the subspace orthogonal to the Ba^+ core.

Equation (14) is used to express the matrix elements $\langle|\mathbf{D}^{\nabla}\cdot\boldsymbol{\epsilon}|\rangle$ occurring in equations (6, 7) in terms of $\langle|\mathbf{D}^{\rm r}\cdot\boldsymbol{\epsilon}|\rangle$. By adding the "rotating" and "counter-rotating" contributions it is possible to show that the length and velocity values of the two-photon Raman coupling are related by:

see equation (18) above.

The contributions of the second, third and fourth terms will be denoted as (a), (b) and (c) respectively, in the following discussion and in Table 3.

The contribution (a) is strictly vanishing for parallel linear polarizations ($\boldsymbol{\epsilon}_1 = \boldsymbol{\epsilon}_2$) due to the equality of the two products. For perpendicular linear polarizations, although the two products introduce different summations, over $J = 1^{\rm e}, 2^{\rm e}$ and over $J = 0^{\rm e}, 2^{\rm e}$ respectively, an almost exact cancelation is obtained (see Tab. 3). Note that in a model where the space spanned by $|E_X J\rangle$ would be complete, this contribution would be proportional to the matrix element $\langle 2|[(\mathbf{r}\cdot\boldsymbol{\epsilon}_2),(\mathbf{r}\cdot\boldsymbol{\epsilon}_1)]|1\rangle$ of the commutator $[\mathbf{r},\mathbf{r}]$, *i.e.* would be strictly equal to zero.

For summations extending over a complete space, the contribution (b) would be proportional to the matrix element of the commutator $[\mathbf{r},\nabla]$:

$$\langle 2|[(\boldsymbol{\nabla}\cdot\boldsymbol{\epsilon}_2),(\mathbf{r}\cdot\boldsymbol{\epsilon}_1)]|1\rangle = \mathcal{N}\langle 2|(\boldsymbol{\epsilon}_2\cdot\boldsymbol{\epsilon}_1)|1\rangle = \delta_{21} = 0, \qquad (19)$$

where $\mathcal{N} = 2$ is the number of active electrons in the frozen-core model. However this equality is not valid in the present calculation. With parallel polarizations, the explicit calculation of the summation involved in the bracket occurring in term (b), is equal to ~ -0.011, leading to the value -0.3 reported in column (b) of Table 3.

The large contribution (c) arises because the "counter-rotating" contribution does not include the ground state $|0\rangle$.

For the diagonal quantities, a similar relation can be written to compare the length $\Omega_{ii}^{\rm r}$ and the velocity $\widetilde{\Omega}_{ii}^{\nabla}$ forms (Eq. (12)) of the dynamical Stark shifts.

The contribution associated with line (a) is strictly vanishing because $\boldsymbol{\epsilon}_1 = \boldsymbol{\epsilon}_2$. The contribution of line (b), which would be equal to the matrix element of the commutator $-(1/\omega^2)[(\boldsymbol{\nabla}\cdot\boldsymbol{\epsilon}),(\mathbf{r}\cdot\boldsymbol{\epsilon})]$ if the summation would include a complete space, *i.e.* would be equal to $-(\mathcal{N}/\omega^2)$ for diagonal matrix elements, is expected to be large in the frozen-core model. Indeed this contribution has to cancel the term proportional to $\mathbf{A}^2$ occurring in the velocity formulation (Eq. (12)). In fact the contribution corresponding to line (b) differs by less than 20% from the value $-(\mathcal{N}/\omega^2)$ reported in the fourth column of this table.

Some numerical values for the real parts of $\widetilde{\Omega}_{ij}^{\nabla}$ and Ω_{ij}^{r}, and for the various contributions to these quantities are given in Table 3, for diagonal and non-diagonal elements. Diagonal quantities with $i = j$ are related only to the shifts due to the laser light ω_k with $k \neq i$.

Equation (18) is numerically verified well, as evident by comparing the *total* contribution $\Re(\Omega_{ij}^{\mathrm{r}})/\sqrt{I_i I_j} + (a) + (b) + (c)$ of the right hand side of this equation to the left hand side $\Re(\Omega_{ij}^{\nabla})/\sqrt{I_i I_j}$.

For the dynamical Stark shifts, the large contributions (b), due to the incompleteness of the subspace spanned using the frozen-core model almost cancel the contribution due to the term $\mathcal{N}\mathbf{A}^2/\omega_k^2$ in equation (12).

On the opposite, for the real part of the two-photon Raman couplings Ω_{21}, the contributions $(a)+(b)$ are small, but the exclusion of the ground state from the "counter-rotating" term (column (c)) is responsible for the difference $\Delta_{21}^{6s} = \pm 16\sqrt{I_1 I_2}$. The resonant contribution of the $|0\rangle$ state to the coupling between the $|1\rangle$ and $|2\rangle$ states is not accounted for in a perturbative way but is dynamically described in the time-dependent evolution of the system. In the rotating wave approximation, this evolution is mainly governed by the one photon Rabi frequencies $\Omega_1 = \langle 1|\mathbf{D}\cdot\boldsymbol{\epsilon}_1|0\rangle\sqrt{I_1}$ and $\Omega_2 = \langle 2|\mathbf{D}\cdot\boldsymbol{\epsilon}_2|0\rangle\sqrt{I_2}$ coupling the states $|0\rangle$, $|1\rangle$ and $|2\rangle$ [16].

Let us emphasize that the difference in the length or velocity values for the Raman-coupling parameters is closely related to the particular excitation scheme employed by Wang *et al.* [14,15] to investigate the possibility of controlling the branching ratios of photoionization products. The two two-color interfering ionization pathways, resonantly enhanced by an intermediate state, proposed in this scheme require only two independent tunable laser fields for populating and ionizing the intermediate resonant states. This control technique is insensitive to the relative phase of the lasers and therefore is very robust, as opposed to schemes using three or four colors which require coherent laser fields [36]. A drawback of this excitation scheme is that the discrete states are necessarily resonantly coupled in a V system, which leads to the difficulty encountered in the definition of "counter-rotating" Raman coupling.

Lastly, it can be pointed out that the velocity formulation gives more rapidly converged results when the size of the reaction volume increases, because it gives higher weight to the part of the wavefunction closer to the nucleus. In the present example, convergence is obtained for the Raman coupling at $r_0 = 40$ a.u. with the velocity form while a value $r_0 = 50$ a.u. is required with the length form.

5 Conclusion

In this paper we have presented a general method to calculate dynamical Stark shifts and two-photon Raman couplings in heavy alkaline-earth atoms. These interactions, which are linear in the intensity of the laser fields (or in the geometrical mean of the two intensities involved in a two-color process) could play a significant role in MPI processes in moderate fields. The approach, based on the jj-coupled R-matrix method combined with MQDT theory, is suitable to account for channel coupling due to electrostatic and spin-orbit interactions and to calculate threshold-resolved one-photon ionization rates even for spin-orbit split thresholds. The application of the method to the study of the dynamics in the coherent control experiment [14,15] will be presented in a forthcoming paper [27].

We have numerically verified that, as formally expected, the imaginary parts of the light shifts and of the Raman couplings, which are respectively equal to the total ionization rates towards "resonant" continua and to the two-photon couplings *via* "resonant" continua, can be obtained in two different ways: (i) explicit calculation of second-order term using the Dalgarno and Lewis method. (ii) determination of the corresponding threshold-resolved quantities, in terms of one-photon dipole matrix elements, followed by a summation over all ionization thresholds. These results emphasize the numerical consistency of the R-matrix approach developed for one- and two-photon processes. This consistency is tightly linked to the fact that the R-matrix introduced in the eigenchannel approach [24] can be expressed in the Wigner-Eisenbud form involving a sum of poles [37]. The same poles appear in the calculation of the "incoming-wave" solutions $|\psi_i^-\rangle$ describing the continuum states of the atom involved in one-photon ionization processes and in the explicit or implicit determination of the Green functions employed to determine two-photon atomic parameters.

Comparison between results obtained using the length or the velocity forms of the electric dipole transition operator, points out the relatively weak influence of using non-complete basis sets in the R-matrix treatment. For atomic states resonantly coupled through the laser lights in a Λ or V system, there is necessarily a difference in the length and velocity form for parameters of second order in the laser field strength. This problem is related to the fact that resonant or non-resonant intermediate states involved in these second order parameters are not treated in the same way.

Such limitations do not appear in the experimental study of two-photon resonant three-photon ionization of barium [11], where the Raman coupling between nearly-degenerate Rydberg states ($6snd\ J = 2$) was found to play a key role. In this process, the Rabi frequencies between the ground state and the $J = 2$ Rydberg states appear to the second-order of perturbation theory and are thus

of the same order of magnitude as the Raman coupling. Moreover no resonant term appears in the calculation of Raman coupling.

The extension of the R-matrix/MQDT method to the determination of Raman couplings between Rydberg states could allow Rydberg wave packet dynamics in two-electron atoms to be studied. Two-photon Raman-like processes are involved in experiments performed with time-delayed pump and probe pulses [38], which have attracted particular interest in recent years.

Numerical calculations were carried out on the Cray 98 belonging to the "Institut de Développement des Ressources en Informatique Scientifique" of the French "Centre National de la Recherche Scientifique". The laboratoire Aimé Cotton is associated with the Université Paris-Sud.

References

1. A.T. Georges, P. Lambropoulos, Phys. Rev. A **18**, 1072 (1978).
2. P.L. Knight, Opt. Commun. **31**, 148 (1979).
3. S.N. Dixit, P. Lambropoulos, Phys. Rev. A **21**, 168 (1980).
4. S.N. Dixit, P. Lambropoulos, P. Zoller, Phys. Rev. A **24**, 318 (1981).
5. G. Alber, P. Zoller, Phys. Rev. A **27**, 1373 (1983).
6. S.N. Dixit, P. Lambropoulos, Phys. Rev. A **27**, 861 (1983).
7. P.L. Knight, M.A. Lauder, B.J. Dalton, Phys. Rep. **190**, 1 (1990).
8. B. Dai, P. Lambropoulos, Phys. Rev. A **36**, 5205 (1987).
9. T. Nakajima, M. Elk, J. Zhang, P. Lambropoulos, Phys. Rev. A **50**, R913 (1994).
10. L.P. Yatsenko, R.G. Unanyan, K. Bergmann, T. Halfmann, B.W. Shore, Opt. Commun. **135**, 406 (1997).
11. J.F. Kelly, J.P. Hessler, G. Alber, Phys. Rev. A **33**, 3913 (1986).
12. L.D. Noordam, H. Stapelfeldt, D.I. Duncan, T.F. Gallagher, Phys. Rev. Lett. **68**, 1496 (1992).
13. D.I. Duncan, R.R. Jones, Phys. Rev. A **53**, 4338 (1996).
14. F. Wang, Ce Chen, D.S. Elliott, Phys. Rev. Lett. **77**, 2416 (1996).
15. F. Wang, D.S. Elliott, Phys. Rev. A **56**, 3065 (1997).
16. T. Nakajima, J. Zhang, P. Lambropoulos, Phys. Rev. Lett. **79**, 3367 (1997).
17. P. Lambropoulos, P. Maragakis, J. Zhang, Phys. Rep. **35**, 203 (1998).
18. M. Cortés, F. Martin, J. Phys. B: At. Mol. Opt. Phys. **27**, 5741 (1994).
19. P. Venuti, P. Declava, A. Lisini, J. Phys. B: At. Mol. Opt. Phys. **29**, 5315 (1996).
20. J. Zhang, P. Lambropoulos, Phys. Rev. Lett. **77**, 2186 (1996).
21. C. Cohen-Tannoudji, J. Dupont-Roc, G. Grynberg, *Photons et atomes : Les processus d'interactions* (InterÉdition, Paris, 1988).
22. P.G. Burke, P. Francken, C.J. Joachain, Europhys. Lett. **13**, 617 (1990).
23. N.J. Kylstra, H.W. van der Hart, P.G. Burke, C.J. Joachain, J. Phys. B: At. Mol. Phys. **31**, 3089 (1998).
24. M. Aymar, C.H. Greene, E. Luc-Koenig, Rev. Mod. Phys. **68**, 1015 (1996).
25. E. Luc-Koenig, A. Lyras, J.-M. Lecomte, M. Aymar, J. Phys. B: At. Mol. Opt. Phys. **30**, 5213 (1997).
26. E. Luc-Koenig, M. Aymar, J.-M. Lecomte, A. Lyras, J. Phys. B: At. Mol. Opt. Phys. **31**, 727 (1998).
27. E. Luc-Koenig, M. Aymar, M. Millet, A. Lyras, J.-M. Lecomte, to be submitted.
28. C.H. Greene, M. Aymar, Phys. Rev. A **44**, 1773 (1991).
29. M.J. Seaton, Rep. Prog. Phys. **46**, 167 (1983).
30. U. Fano, A.R.P. Rau, *Atomic Collisions and Spectra* (Academic, Orlando, 1986).
31. P. Camus, M. Dieulin, A. El Himdy, M. Aymar, Phys. Scripta **27**, 125 (1983).
32. J.-M. Lecomte, M. Telmini, M. Aymar, E. Luc-Koenig, J. Phys. B: At. Mol. Phys. **27**, 667 (1994).
33. M. Aymar, J.-M. Lecomte, J. Phys. B: At. Mol. Opt. Phys. **22**, 223 (1989).
34. A. Dalgarno, J.T. Lewis, Proc. R. Soc. **233**, 70 (1955).
35. C. Cohen-Tannoudji, J. Dupont-Roc, G. Grynberg, *Photons et atomes : Introduction à l'électrodynamique quantique* (InterÉdition, Paris, 1987).
36. Z. Chen, P. Brumer, M. Shapiro, J. Chem. Phys. **98**, 6843 (1993).
37. F. Robicheaux, Phys. Rev. A **43**, 5946 (1991).
38. H. Henle, H. Ritsch, P. Zoller, Phys. Rev. A **36**, 683 (1987).